

Optical metrology for very large convex aspheres

J. H. Burge, P. Su, and C. Zhao

College of Optical Sciences, University of Arizona, Tucson, AZ 85721, USA

ABSTRACT

Telescopes with very large diameter or with wide fields require convex secondary mirrors that may be many meters in diameter. The optical surfaces for these mirrors can be manufactured to the accuracy limited by the surface metrology. We have developed metrology systems that are specifically optimized for measuring very large convex aspheric surfaces. Large aperture vibration insensitive sub-aperture Fizeau interferometer combined with stitching software give high resolution surface measurements. The global shape is corroborated with a coordinate measuring machine based on the swing arm profilometer.

Keywords: Aspheres, optical fabrication, optical testing, large optics

1. INTRODUCTION

Giant telescopes are being developed that require convex aspheric secondary mirrors many meters in diameter. Measurement techniques implemented in the last decade have allowed fabrication of secondary mirrors up to 1.7 meter in diameter. Today's new giant telescopes are considering secondary mirrors up to 4 meters in diameter. Three of these are listed in Table 1. This paper presents techniques for measuring these large mirrors to the accuracy required by the advanced optical telescopes.

Table 1. Giant telescopes that have proposed to use very large convex secondary mirrors

Telescope	LSST ¹	TMT ²	European-ELT ³
Primary mirror diameter	8.4 m	30 m	42 m
Secondary mirror diameter	3.4 m	3.1 m	6 m
Secondary mirror radius of curvature	6.79 m	6.2 m	15.5 m
Secondary mirror conic constant	-0.22 + aspheric terms	-1.32	-2.39
Secondary aspheric departure	17 μm	$\sim 900 \mu\text{m}$	$\sim 1600 \mu\text{m}$

As with all optical surfaces, the control of the shape accuracy is determined primarily by the quality of the measurement system. Mirrors with spherical surfaces may be measured accurately using the spherical symmetry – the curvature is the same at all places on the surface. The measurement of aspheric surfaces is more difficult. Large concave aspheric mirrors can be readily measured with an interferometer and null corrector located near the center of curvature of the mirror.⁴ The concave shape allows the optical system to be small compared to the mirror being measured. Convex aspheric mirrors are more difficult.

The classic test for convex secondary mirrors is the Hindle test, which requires an auxiliary mirror much larger than the mirror being measured. A variation of this uses a Hindle shell, which is only as large as the mirror being measured, but has accuracy that is limited by the transmission quality of the glass. Both tests are performed over large paths and are susceptible to problems from vibrations or air motion. All of these problems are solved using a Fizeau interferometric test⁵ that uses either an aspheric reference surface or a spherical reference surface with computer generated hologram CGH⁶. These tests have been highly successful for large secondary mirrors, up to 1.7-m in diameter.⁷

These full aperture tests are limited by the glass substrates used to provide the references. We propose to measure very large secondary mirrors using sub-aperture Fizeau interferometry. The data can be combined to provide a full aperture map. The low order shape errors can be corroborated with a coordinate measuring machine based on swing arm profilometry.

jburge@optics.arizona.edu; phone 520-621-8182, fax 520-621-3389

This paper discusses the issues for performing sub-aperture Fizeau interferometry and for stitching the data. We also present the design of an optical coordinate measuring machine that uses a swing arm profilometer with optical probes. Examples of systems for measuring the LSST and TMT secondary mirrors are presented.

2. MEASUREMENTS USING SUB-APERTURE FIZEAU INTERFEROMETRY

Fizeau interferometry provides accurate measurements with excellent spatial resolution. As stated above, it is impractical to measure the full aperture with a single test plate. Sub-apertures can be measured with test plates that are much smaller than the mirror being measured. Data from the sub-apertures can be stitched together to provide the full aperture map required to guide fabrication or to qualify the finished surface.

We propose to use aspheric Fizeau reference plates that are ~1 m in diameter. This size allows a balance of test efficiency, performance, and cost. We use an aspheric reference rather than a CGH for two reasons:

- The non-axisymmetric CGH would be difficult to fabricate on the curved reference surface
- The aspheric test allows simultaneous phase shifting which makes the test insensitive to vibration, which relaxes requirements for the mechanical systems.

The layout for a test of a 1.7-m secondary mirror with a 1-m sub-aperture aspheric Fizeau test plate is shown in Figure 1. The full surface is measured by rotating the secondary mirror under the sub-aperture test plate.

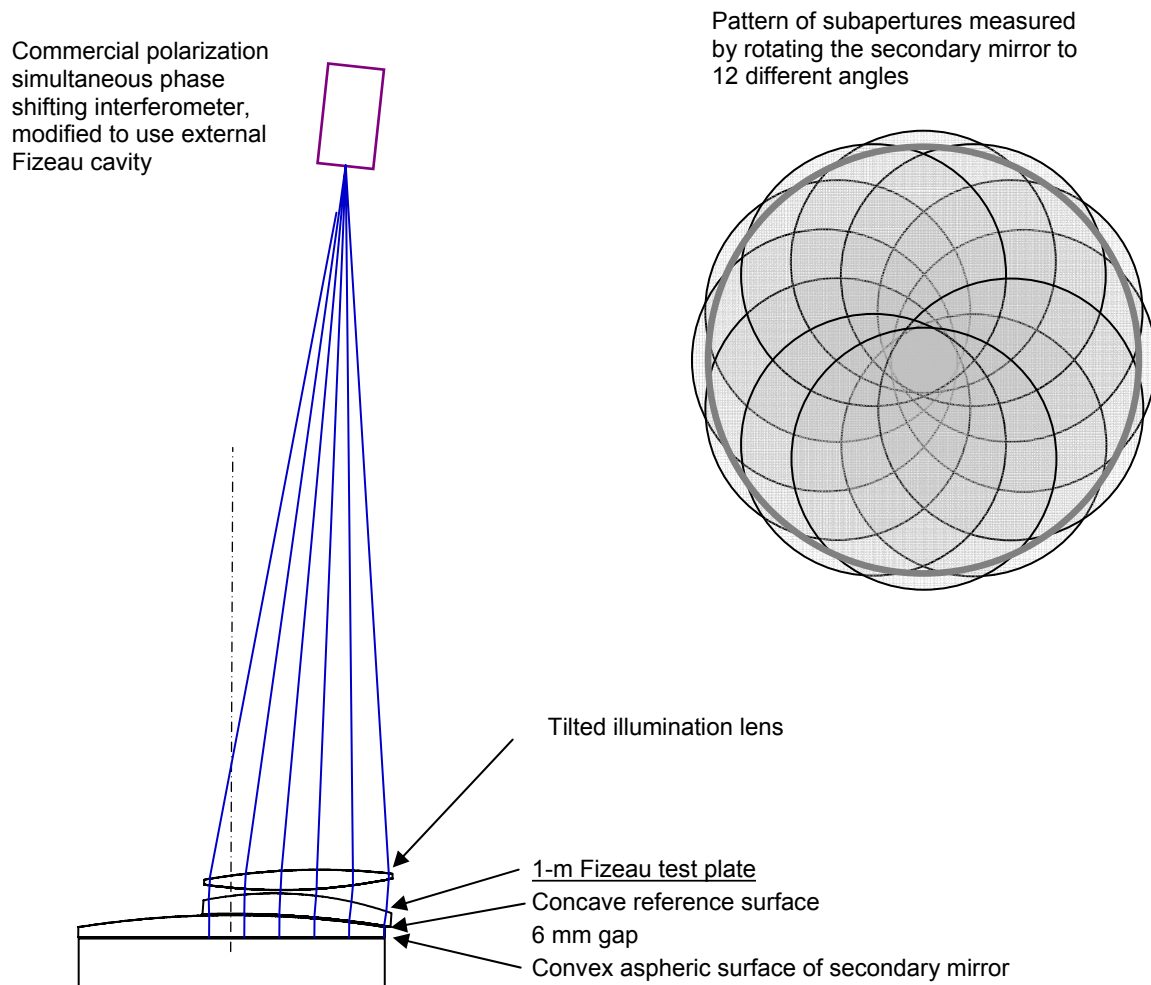


Figure 1. Layout of Fizeau test for a 1.7-m convex asphere using a 1-m concave reference.

2.1 Sensitivity of Fizeau test to errors

The Fizeau interferometer uses reflection from the reference surface that is held only a few mm from the surface being measured. The reflection from the reference surface interferes with light reflected from the surface under test, and the difference between the two reflected wavefronts is used for the measurement. Phase shifting interferometry can be performed by either pushing the reference plate with piezoelectric transducers or using a simultaneous phase shifting interferometer that uses polarization to separate the reflections. We use the polarization simultaneous phase shifting for large Fizeau tests. The details of this are discussed below.

It is important to understand that the Fizeau measurement compares the reference surface with the surface being measured. Other optics, such as the illumination lens, do not contribute directly to the measurement error. The illumination optical system, which consists of the illumination lens, the back (convex) surface of the test plate and the test plate glass are used to bring the rays of light so they are nominally normal to the reference surface (and thus the convex surface being measured.) Departure from normal causes only a cosine effect, which is quite weak. The tolerances for the illumination optics and the simulated effects on the system performance are shown in Table 2. The tolerances are very loose, and yet the effect on the measurement accuracy is on 0.6 nm rms!

Table 2. Coupling between errors in the illumination system and the resulting errors in the SM surface measurement

	nominal value	Tolerance	units	mrad rms
<u>Fizeau Test plate</u>				
TP S2 RoC	1960	20	mm	0.049
TP thickness	100	3	mm	0.005
TP S2 irregularity		0.1	mrاد	0.050
TP-IL spacing	24	3	mm	0.000
<u>Illumination lens</u>				
IL x tilt	5.74	0.2	deg	0.061
IL y tilt	0	0.2	deg	0.061
IL clocking	0	0.5	deg	0.018
IL dx	0	3	mm	0.029
IL dy	0	3	mm	0.028
IL thickness	108	3	mm	0.003
IL S1 RoC	2863	24	mm	0.033
IL S1 conic	-6.48	0.4		0.076
IL S2 RoC	3476	12	mm	0.121
S1 irregularity		0.5	mrاد	0.250
S2 irregularity		0.2	mrاد	0.100
Design residual				0.087
RSS wavefront slope			mrad rms	0.345
Effect on surface error			nm rms	0.6

The primary source of error in the Fizeau test comes from uncertainty in the reference surface. For an aspheric reference, we measure this concave off-axis aspheric surface with accuracy of ~3 nm rms using an interferometer with CGH null corrector. An error budget for the Fizeau measurements is presented in Table 3.

Table 3. Error budget for Fizeau test

Error source	nm rms	Comment
Illumination optics	0.6	See Table 2
Accuracy of aspheric reference surface map	2.9	(Further mitigation using over sampling)
Measurement errors from CGH	2.5	Phase etched CGH, limitation for correction of substrate errors
CGH Substrate calibration	1.9	0.003 λ rms (1% duty cycle, 2% etch variation) ⁸
CGH distortion	1.3	0.002 λ rms (0.03 μ m rms pattern distortion, 15 μ m pitch)
Residual noise, interferometer calibration	1.0	
Residual from interferometer, noise	1.0	Requires careful calibration, averaging
Distortion from mounting for test	1.0	Measure <i>in situ</i> , any change is mostly astigmatism
Mapping of reference surface errors	1.2	6 nm/cm rms slope, 2 mm mapping
Substrate distortion for mounting in operation	1.0	Measure <i>in situ</i> , use over sampling to mitigate
Noise from measurement	1.0	Low noise, average multiple maps
RSS for sub-aperture measurement	3.5	

The numbers reported above do not contribute directly to the measurement of the secondary mirrors because we over sampled by a factor of about 2 as shown in Figure 1. The noise in the measurements is reduced by 30%. Also, we isolate errors in the reference surface as those that stay fixed with the reference surface. Nonetheless, we adopt 3 nm rms as our budgetary number for the sub-aperture measurement accuracy. The overall surface accuracy is determined by the stitching algorithm, which is discussed below.

2.2 Simultaneous phase shifting Fizeau test interferometer

Phase shifting interferometry PSI is used to obtain high resolution, accurate surface data from the interferograms. Traditional PSI uses sequential frames that are measured as the relative phase is shifted, nominally 90° per frame. This method has been very successful, but it suffers from sensitivity to vibrations. A measurement error occurs if the interferogram vibrates so that the frames are not 90° apart. This is solved using simultaneous phase shifting interferometry where the phase shifted frames are taken at the same time. Commercial Fizeau interferometers that use a combination of tilt and polarization for simultaneous phase shifting are now available from 4D Technologies and ESDI. Although these machines are made to operate with an attached Fizeau reference, we can modify them to function with our reference.

The simultaneous phase shifting interferometer uses two beams with orthogonal polarization with some tilt difference. These two are each reflected from the reference surface and from the surface under test. By setting the relative tilts for the optics, one can select the reference and test beam with appropriate orthogonal polarizations. Then the phase shifting is performed using polarization optics to create 3 or 4 interferograms that have 90° relative phase shift and can be read out simultaneously. The wavefront phase is then calculated from the set of interferograms.

As long as the physical separation is small, then the effects of imperfect wavefronts due to limitations in the illumination optics and the test plate glass do not significantly affect the measurement. A general analysis for such errors is given by Burge⁹. Also, the effect of birefringence in the test plate has been shown to have negligible effect for the simultaneous phase shifting interferometers as long as circular polarization is used.¹⁰

The use of a commercial vibration insensitive Fizeau interferometer with the remote test plate was demonstrated for 1-m aperture measurements.¹¹ This system used the H-1000 instantaneous Fizeau system from ESDI and included an off-axis parabola for illumination. Measurements achieve a noise level of 3 nm rms over the 1-m aperture.

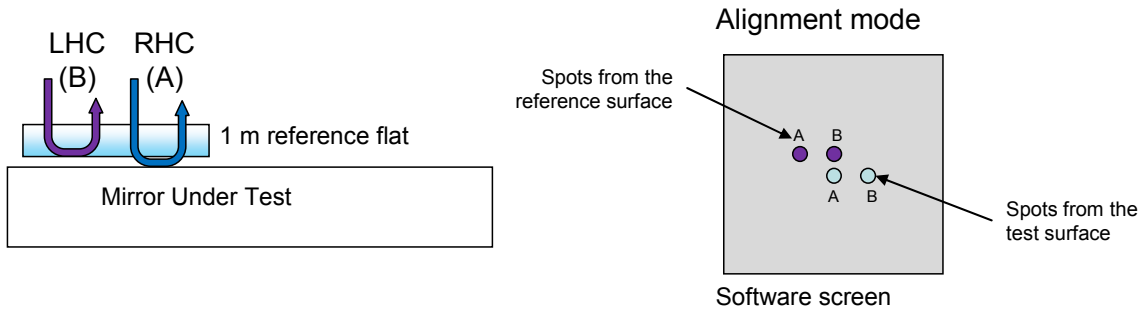


Figure 2. Layout of Fizeau test for sub-aperture interferometric measurement of a flat mirror. Two wavefronts with different tilt and polarization are emitted by the interferometer. The reference and test are aligned so that the reference beam with polarization state B coincides with the test wavefront with polarization A. Polarization optics are then used to create multiple images with different relative phase shift between them.

2.3 Stitching sub-aperture data

Measurements with ~ 2 nm accuracy have been performed with a vibration insensitive 1-m aperture Fizeau simultaneous phase shift interferometer¹² of the type described above. The second development required for the large secondary mirror measurements is the ability to stitch sub-aperture data. We have developed software for performing this analysis using two methods:

- **Modal solution**¹³: We define the measured surface, the reference surface, and the alignment as a number of modes. We use the least squares method to solve for the modes that provide optimal consistency with the data. We use singular value decomposition to define the modes that we consider. This has the advantage of solving for errors in the reference surface as well as the surface being measured.
- **Stitching**^{14,15}: We maintain the full resolution data and use least squares to solve for the alignment degrees of freedom (tip/tilt and piston for a flat, additional terms for the aspheres). This has the advantage of creating a complete map that maintains measurement resolution.

A 1.6-m mirror was measured using a 1-m sub-aperture vibration insensitive Fizeau system. Figure 3 shows the geometry used for these measurements as well as the reconstructed reference surface figure determined from the modal solution. Figure 4 compares the modal solution of the 1.6-m flat mirror with the solution from stitching. The difference between the two appears only as high order variations that were not included in the modal solution.

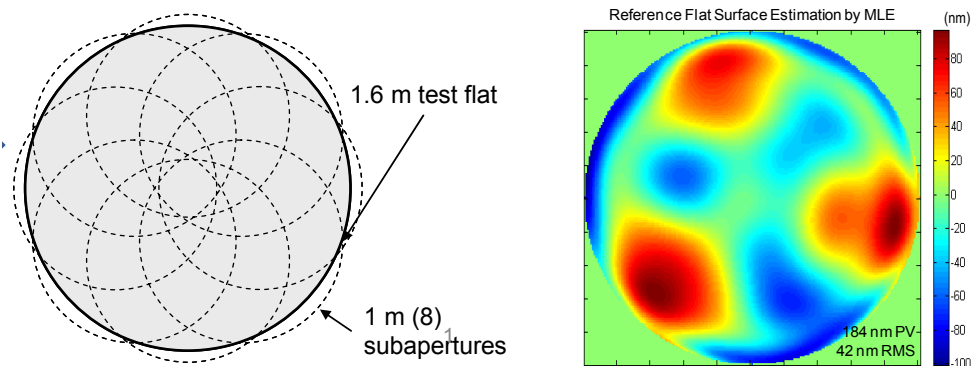


Figure 3. The 1.6-m mirror was measured using 8 sub-aperture measurements with a 1-m Fizeau test plate with polarization simultaneous phase shifting. The modal solution (maximum likelihood estimate) provided the shape of the reference surface, shown here as 42 nm rms. This shape was expected from the support error and from the polishing residual.

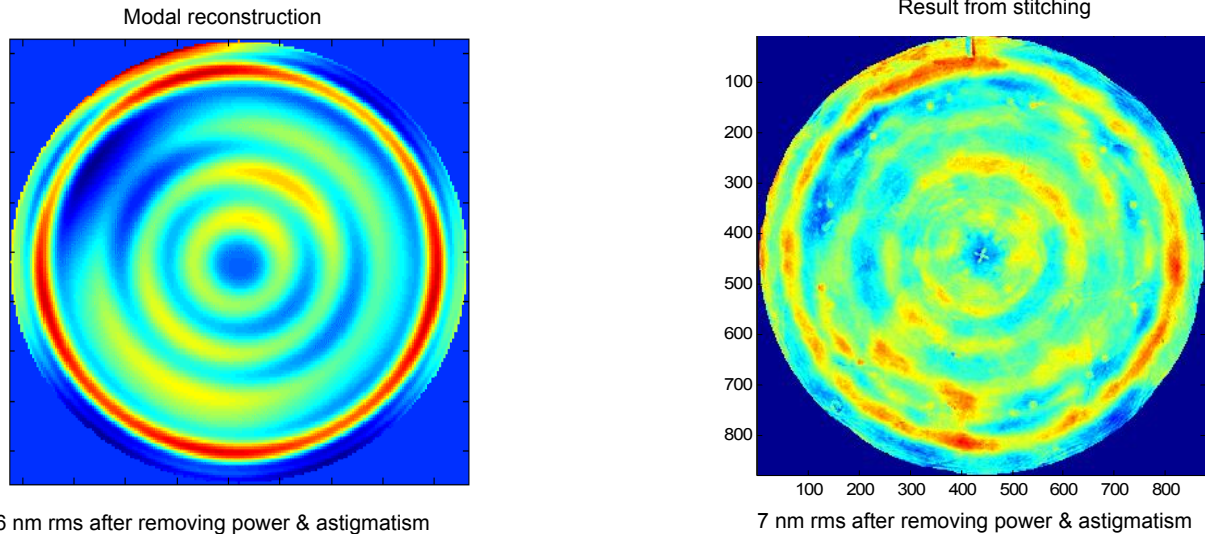


Figure 4. Sub-aperture data for a 1.6 m mirror that were reduced two different ways, modally where Zernike coefficients are optimized to provide consistency with the data, and by direct stitching where the individual maps are used directly, with adjustments in tilt and piston.

3. FIZEAU TEST OF GIANT SECONDARY MIRRORS

3.1 LSST secondary mirror

The 3.4-m diameter secondary mirror for LSST can be readily measured with the Fizeau method. The mirror itself is 3.4 meters in diameter, but because of its large central hole, it can easily be measured with a single Fizeau test plate. Since only one test plate is needed, this test can be performed using much of the existing equipment at the University of Arizona from the 1.6-m test. The layout for LSST testing is shown in Figure 5.

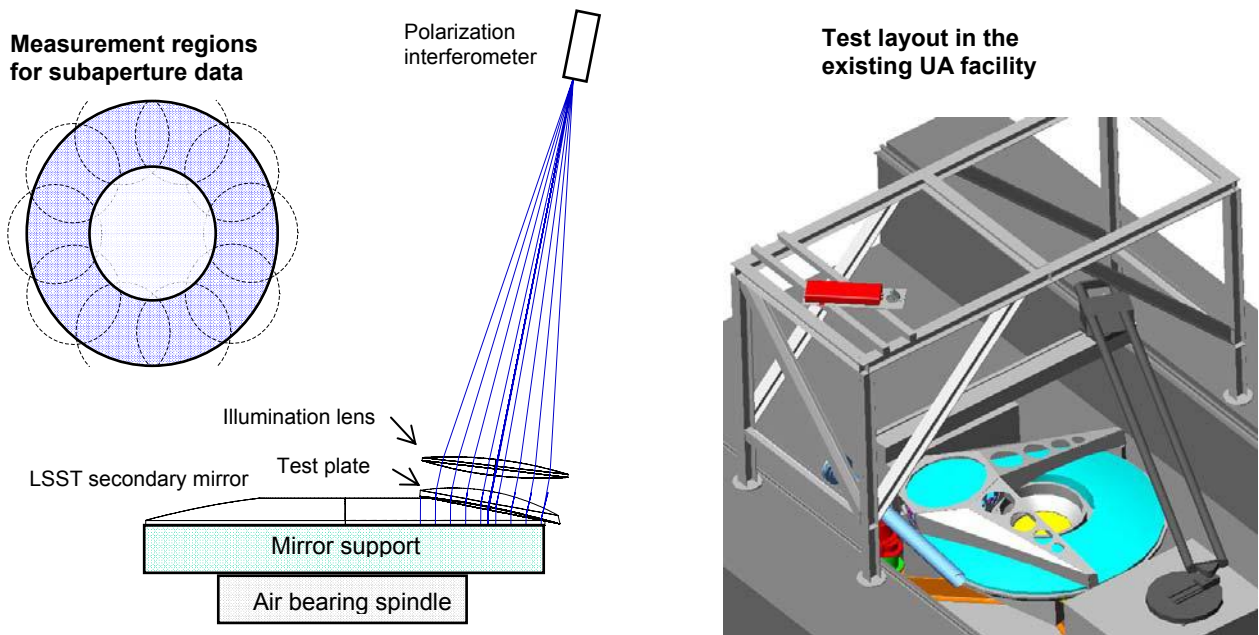


Figure 5. Layout for LSST secondary mirror test in the Optical Sciences shop at University of Arizona

3.2 TMT secondary mirror

The 3.1-m secondary for the TMT is more interesting. As this does not have a large central hole, two different test plates are required. We use one meter sub-apertures, located with their centers 45 and 115 cm from the center of the secondary mirror as shown in Figure 6. The convex secondary mirror is highly aspheric, so the Fizeau reference plates must be made with matching concave aspheric surfaces. These can be individually manufactured as off-axis aspheres and can be measured from center of curvature using an interferometer with computer generated hologram. The hologram itself can be used for the alignment of the test.¹⁶ The aspheric departure for the concave test plates are shown in Figure 6.

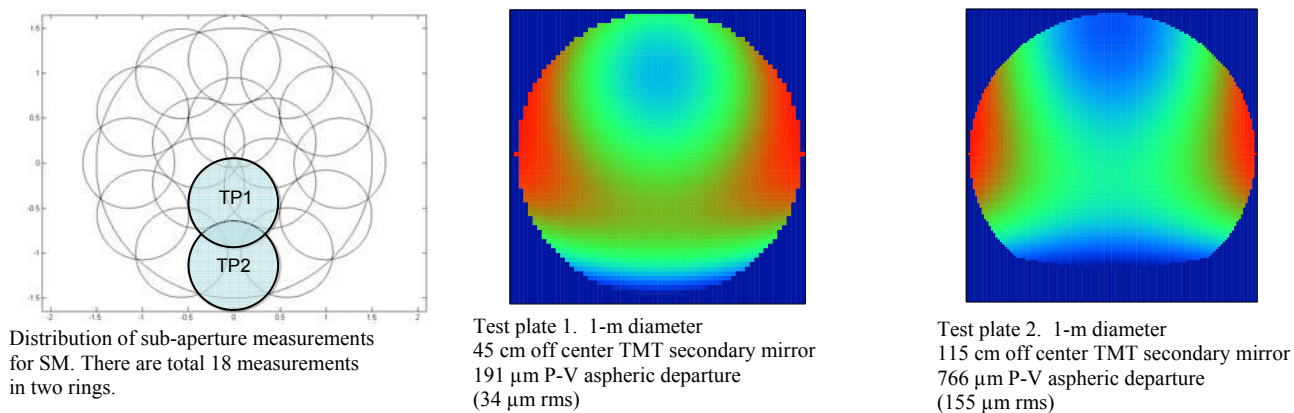
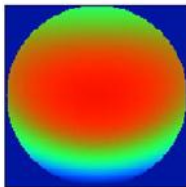
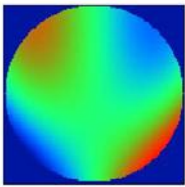
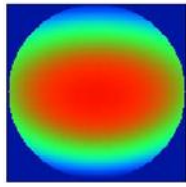
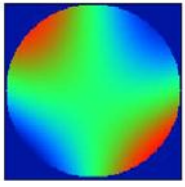


Figure 6. Layout and aspheric departure for the test plates for the Fizeau test of the TMT secondary mirror.

Stitching of TMT interferometry data

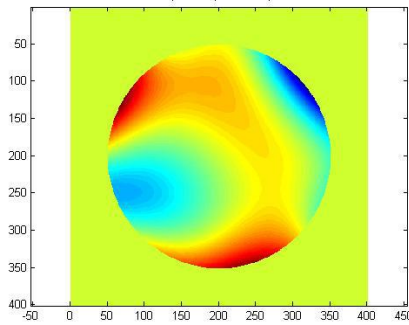
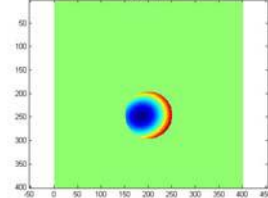
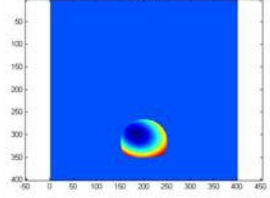
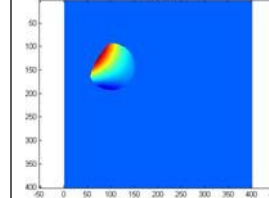
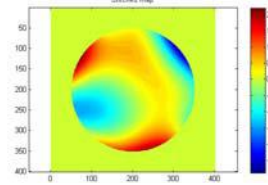
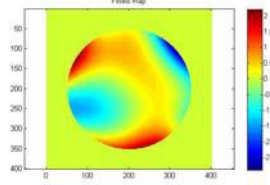
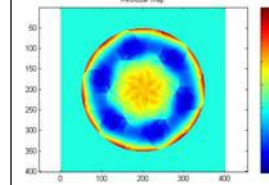
A complete simulation was performed for the measurement of the TMT secondary mirror using 18 sub-apertures. The tip, tilt, piston, and power for the sub-apertures must be fit. In addition, there are two alignment modes per measurement that must be fit – radial motion of the test plate and clocking of the test plate about its local axis. The effects of these degrees of freedom are shown below in Table 4. In this analysis, the alignment errors for radial position and clocking are assumed to be constant for the test – *i.e.* they have the same value for all measurements. The tip, tilt, piston, and power are assumed to be independent for all 18 sub-aperture measurements.

Table 4. The apparent wavefront errors when the reference mirrors have alignment errors relative to SM.

	Radial shift 1mm	Clocking 0.05 degree
Test plate 1	 <p>Zernike standard coefficients (rms nm): Z4 (power): -173 Z6 (0° astigmatism): 122 Z7 (90° coma): 38</p>	 <p>Zernike standard coefficients (rms nm): Z5 (45° astigmatism): -48 Z8 (0° coma): 15</p>
Test plate 2	 <p>Zernike standard coefficients (rms nm): Z4 (power): -407 Z6 (0° astigmatism): 278 Z7 (90° coma): 28</p>	 <p>Zernike standard coefficients (rms nm): Z5 (45° astigmatism): -298 Z8 (0° coma): 36</p>

The complete stitching algorithm was developed for TMT and demonstrated using two simulations. The first simulation shows the ability of the stitching to reconstruct a particular figure error. Synthetic data were created for the secondary mirror and random alignment errors were included for the sub-aperture (SA) measurements. For this case, in the absence of noise, the stitching is perfect, as shown in Table 5. This was repeated for each of the Zernike terms. The second simulation was a Monte Carlo type simulation that demonstrates the ability of the algorithm to reject noise.

Table 5. Simulation for stitching 18 maps together, including alignment errors, to recreate the secondary mirror surface.

<p>Given SM full aperture map:</p>	<p>Input full aperture map: 0.747μm rms (synthetic data)</p> 		
<p>Example SA measurements: Ref radial shift and clocking: Ref1: 0.25mm, 0.025° Ref2: -0.25mm, -0.025° Random power of 1μm sigma added to each SA measurements</p>	<p>SA measurement 1: 0.460μm rms</p> 	<p>SA measurement 2: 0.737μm rms</p> 	<p>SA measurement 3: 0.604μm rms</p> 
<p>Stitching result: reference alignment error REMOVED</p>	<p>Stitched map: 0.747μm rms</p> 	<p>Fitted map: 0.747μm rms</p> 	<p>Residual from Fit: 0.001μm rms</p> 

To determine the effect of noise, we stitched data together where the data had only noise. The resulting map shows the effect of noise. The noise was modeled with as 3 nm rms surface error with correlation length equal to about 1/4 the diameter of the 1-m sub-aperture. A typical plot of the noise is shown in Figure 7. The noise for each sub-aperture measurement was independent. The surface was then reconstructed from the sub-aperture data and evaluated. An example from one of the Monte Carlo trials is shown in Figure 8.

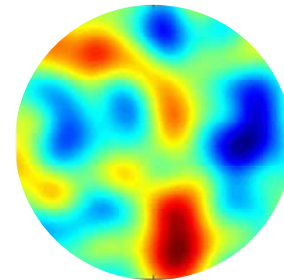


Figure 7. Typical noise for the 1-m sub-aperture measurements of 3 nm rms with correlation length about 0.25 meter.

In the simulations, we used 100x100 pixels for each sub-aperture and 300x300 pixels for the full M2 aperture. The actual matrix for the full-aperture map is 400x400 pixels. We ran 50 Monte Carlo simulations of stitching sub-aperture measurements with 3nm correlated noise. We fitted the stitched maps to the 11 modes (equivalent to 2 Zernike astigmatisms, 2 trefoils, 1 focus, 2 quadfoils, 2 comas and 2 pentafoils (see Figure 9) and obtained statistics for the fitted coefficients of the modes. Because the axial alignment of the reference mirrors affects the power measurement of sub-apertures, there is uncertainty in determining the power of the stitched surface map such that the power is indeterminate. The real power in the surface would be measured by controlling the spacing from the test plate to the mirror for one of the measurements.

Stitched map: 8.2nm rms

11-term Zernike fit to stitched map:
6.4nm rms

Residual from fit: rms 3nm

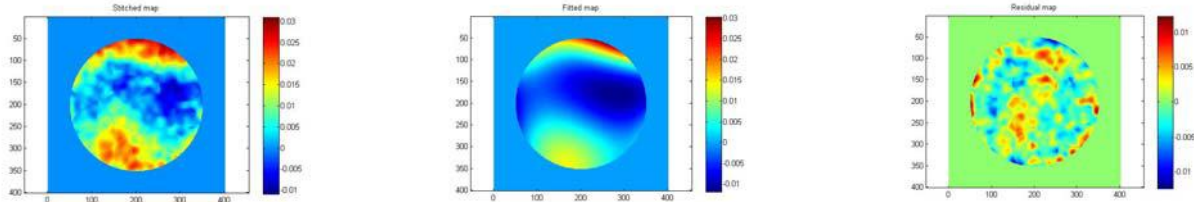


Figure 8. Example for one of the Monte Carlo runs which includes the effect of 3 nm rms noise per measurement.

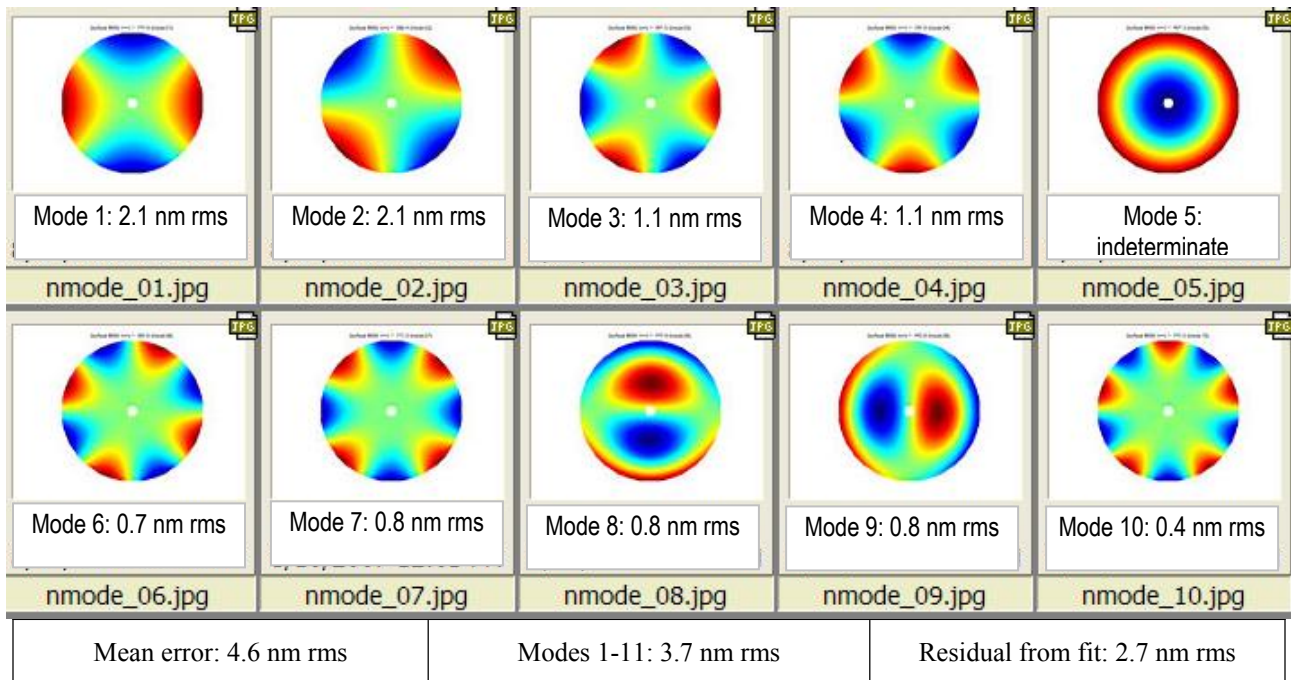


Figure 9. Results of fitting a 50 trial Monte Carlo simulation to TMT SM modes, represented as Zernikes. Each of the 18 measurements was simulated to have random misalignment as well as 3 nm rms random error as shown in Figure 7.

4. SWING ARM OPTICAL CMM

A second test for the secondary mirrors uses a coordinate measuring machine (CMM) called the swing arm profilometer¹⁷, which utilizes advantageous geometry for measuring the optical surface. The swing arm profilometer uses a displacement probe at the end of an arm to make mechanical measurements of the optical surface. The geometry for this test is shown in Figure 10. This geometry can be used to make scans across the diameter of the surface. Multiple scans can be combined by using data from circumferential scans, made by rotating the substrate under the probe.

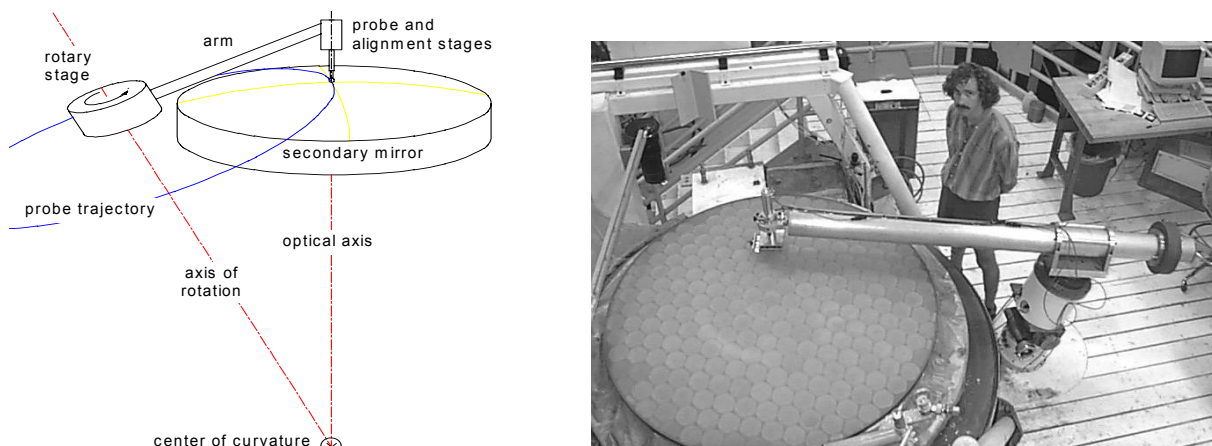
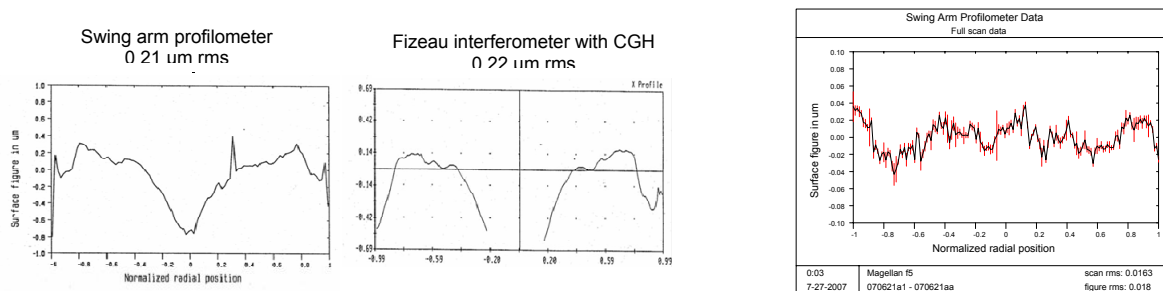


Figure 10. The swing arm profilometer measures along arcs on the surface by pivoting an arm about an axis that goes through the center of curvature of the mirror being measured. A probe at the end stays normal to the surface and measures only the aspheric departure. This geometry works equally well for concave and convex measurements, such as the measurement of the 1.7-m convex mirror shown here.

The University of Arizona has used the swing arm profilometer to provide surface measurements with accuracy of $\sim 0.05 \mu\text{m}$ rms for meter sized convex aspheres *without calibrating the bearing*. Figure 11 shows a comparison of a profilometer measurement with results from a full aperture Fizeau test with CGH. Since these measurements were made, the mechanical probe has been replaced by a non-contact optical probe that provides $\sim 2 \text{ nm}$ resolution and higher data rates since the arm is swept continuously. The mechanical probe required the machine to step and settle between sample points, taking ~ 2 seconds per point.



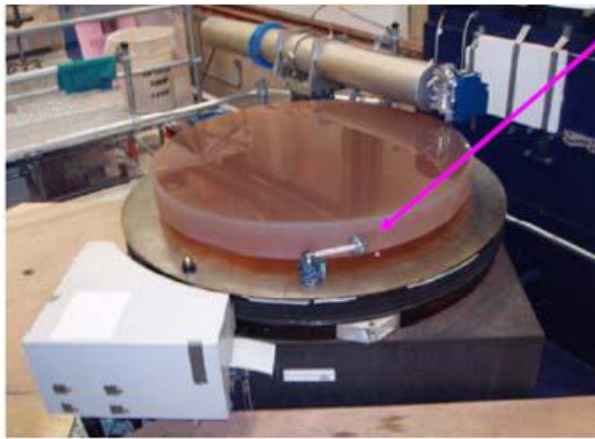
Noise in a single scan of 18 nm rms. This is measured by subtracting the average of many scans from a single scan

Figure 11. The swing arm profilometer achieves excellent accuracy without even calibrating the air bearing. The comparison between profilometer measurements and interferometry is excellent. Noise of 18 nm rms for a single scan of a 1.7-m convex asphere is shown.

The swing arm optical CMM (SOC) was created by adding two significant improvements to the swing arm profilometer:

- The touch probe was replaced by an optical probe. This allows non-contact measurements with a continuously scanning arm, allowing much more rapid data collection.
- The part is rotated on a high quality rotation air bearing. This allows accurate combination of the scans, providing full aperture data.

These improvements, along with some data, are shown in Figure 12. The machine shows arc scans with 60 nm rms repeatable variation that can be calibrated and 30 nm rms non-repeatable errors. The table scans have random errors of 30 nm rms.



SOC measuring 1.5-m convex asphere

Swingarm scans

Repeatable errors of 60 nm rms
Non-repeatability of 30 nm rms

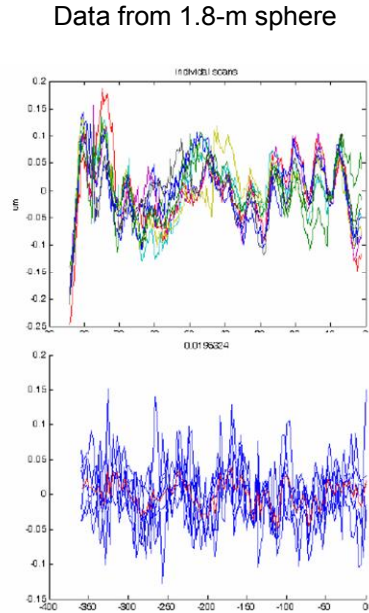


Table rotation

Random errors of 30 nm rms

Figure 12. The Swing arm Optical CMM is shown here with a 1.5-m convex optic. Some data from arc scans and table scans from a good 1.8-m sphere are also shown.

The accuracy of making full surface measurements for the TMT secondary was modeled for the swing arm profilometer assuming measurement noise of 0.1 μm rms per point. A Matlab program was written to process the measurement data. The data is fit to low order Zernikes which are close to the M2's natural modes.

A Monte Carlo simulation of the swing arm profilometer was performed assuming 0.1 μm uncertainty at each measurement point. With 6 scans (4 radial scans and 2 circumferential scans) and 200 points per scan, the average uncertainty in the lowest 11 modes is less than 15 nm. We also investigated the sensitivity to the number of scans by direct simulation. Figure 13 shows the dependence of the noise as functions of the number of scans/measurement and the number of Zernike terms in the fit. The larger number of scans improves performance in two ways:

- The data density is higher, so the sampling is better.
- More points are measured, so the noise is reduced by averaging.

The performance is plotted as functions of the number of modes fit and the number of scans made in Figure 13. For the case of measuring all 11 modes, ten scans (8 diameters and 2 circumferential) can determine the surface to 13 nm rms. These numbers are achievable for a system with performance similar to that of the University of Arizona machine. This was a custom built machine which could be duplicated. Clearly the ultimate performance for any machine will depend on the quality of the engineering and the components.

It is difficult to measure the radius of curvature using the swing arm profilometer. A misalignment of the arm appears as power in the scan. The radius of curvature corroboration requires a different test.

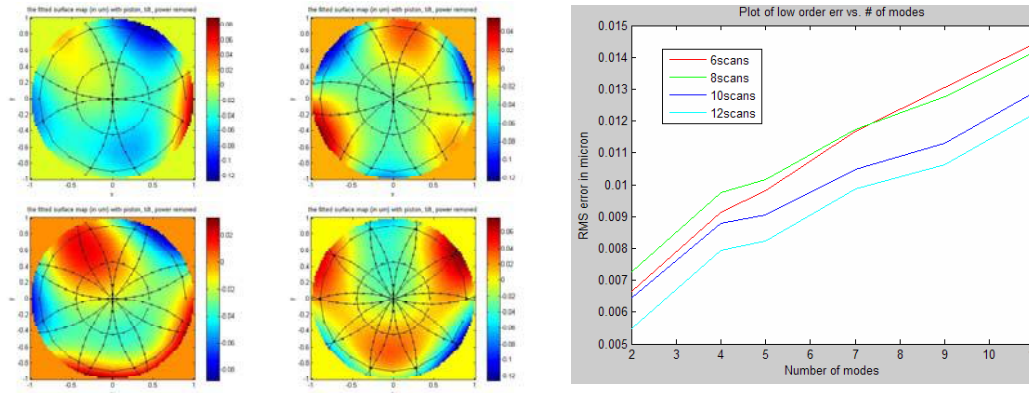


Figure 13. Monte Carlo analysis of M2 measurements with a swing arm profilometer with 0.1 μm noise per measurement point. Different scan configurations are included here.

5. CONCLUSION

Until recently, the possibility of a giant convex aspheric mirror that extends many meters in diameter was unthinkable. The University of Arizona has developed and implemented metrology methods that are directly scalable to such mirrors. This measurement capability, coupled with the proven techniques of large tool grinding and computer controlled polishing enable the University of Arizona to manufacture large convex aspheres as large as 8 meters with proven equipment.

REFERENCES

- 1) S. Olivier, L. Seppala, K. Gilmore, L. Hale, W. Whistler "LSST camera optics," *Optomechanical Technologies for Astronomy*, edited by E. Atad-Ettingui, J. Antebi, D. Lemke, Proc. SPIE **6273**, 62730Y, (2006)
- 2) M. K. Cho, "Performance prediction of the TMT secondary mirror support system," in *Advanced Optical and Mechanical Technologies in Telescopes and Instrumentation*, ed. E. Atad-Ettingui and D. Lemke, Proc. SPIE 7018 (2008; these proceedings).
- 3) D. Enard, *et al.*, "Report of ELT Telescope Design Working Group-28/02/2006," (2006).
- 4) J. H. Burge, *Advanced Techniques for Measuring Primary Mirrors for Astronomical Telescopes*, Ph. D. Dissertation, Optical Sciences, University of Arizona (1993).
- 5) J. H. Burge, "Fizeau interferometry for large convex surfaces," in *Optical Manufacturing and Testing*, V. J. Doherty and H. P. Stahl, Editors, Proc. SPIE **2536**, 127-138 (1995).
- 6) J. H. Burge and D. S. Anderson, "Full-aperture interferometric test of convex secondary mirrors using holographic test plates," in *Advanced Technology Optical Telescopes V*, L. M. Stepp, Editor, Proc. SPIE **2199**, 181-192 (1994).
- 7) B. K. Smith, J. H. Burge, H. M. Martin, "Fabrication of large secondary mirrors for astronomical telescopes" in *Optical Manufacturing and Testing II*, H Stahl Ed., Proc. SPIE **3134**, 51-61 (1997).
- 8) P. Zhou and J. H. Burge, "Optimal design of computer-generated holograms to minimize sensitivity to fabrication errors," *Opt. Express* **15**, 15410-15417 (2007).
- 9) J. H. Burge, "Fizeau interferometry for large convex surfaces," in *Optical Manufacturing and Testing*, V. J. Doherty and H. P. Stahl, Editors, Proc. SPIE **2536**, 127-138 (1995).
- 10) C. Zhao, D. Kang, and J. Burge, "Effects of birefringence on Fizeau interferometry that uses a polarization phase-shifting technique," *Applied Optics* **44**, 7548-7553 (2005).
- 11) C. Zhao, R.A. Sprowl, M. Bray, J.H. Burge, "Figure measurement of a large optical flat with a Fizeau interferometer and stitching technique," in *Interferometry XIII*, edited by E. Novak, W. Osten, C. Gorecki, Proc. of SPIE **6293**, 62930K, (2006).
- 12) Yellowhair, P. Su, M. Novak, J. Burge, "Fabrication and testing of large flats," in *Optical Manufacturing and Testing VII*, ed. by J. Burge, O. Faehnle, and R. Williamson, Proc. SPIE **6671**, (2007).
- 13) P. Su, J.H. Burge, R. Sprowl, J. Sasian, "Maximum Likelihood Estimation as a General Method of Combining Sub-Aperture Data for Interferometric Testing," in *International Optical Design Conference 2006*, Proc. SPIE **6342** (2006).
- 14) M. Otsubo, K. Okada, J Tsujiuchi, "Measurement of large plane surface shapes by connecting small aperture interferograms," *Optical Engineering*, **33** (2), 608-613, (1994).
- 15) M. Bray, "Stitching interferometer for large plano optics using a standard interferometer", in *Optical Manufacturing and Testing II*, ed. H. P. Stahl, Proc. SPIE **3134**, 39-50. (1997).
- 16) J. H. Burge, R. Zehnder, C. Zhao, "Optical alignment with computer-generated holograms," in *Optical System Alignment and Tolerancing*, ed. by J. Sasian and M. Ruda, Proc. SPIE **6676**, (2007).
- 17) D. S. Anderson and J. H. Burge, "Swing arm profilometry of aspherics," in *Optical Manufacturing and Testing*, V. J. Doherty and H. P. Stahl, Editors, Proc. SPIE **2536**, 169-179 (1995).